UCLA
UCLA Previously Published Works

Title

The Orphan Nuclear Receptor Nur77 Is a Determinant of Myofiber Size and Muscle Mass in Mice

Permalink

https://escholarship.org/uc/item/154458j9

Journal

Molecular and Cellular Biology, 35(7)

ISSN

0270-7306

Authors

Tontonoz, Peter
Cortez-Toledo, Omar
Wroblewski, Kevin
et al.

Publication Date

2015-04-01

DOI

10.1128/mcb.00715-14

Peer reviewed

The Orphan Nuclear Receptor Nur77 Is a Determinant of Myofiber Size and Muscle Mass in Mice

Peter Tontonoz,[a,b] Omar Cortez-Toledo,[c] Kevin Wroblewski,[a] Cynthia Hong,[a] Laura Lim,[c] Rogelio Carranza,[c] Orla Conneely,[d] Daniel Metzger,[e] Lily C. Chao[a,c,f]

Department of Pathology and Laboratory Medicine, David Geffen School of Medicine, University of California at Los Angeles, Los Angeles, California, USA[a]; Howard Hughes Medical Institute, University of California at Los Angeles, Los Angeles, California, USA[b]; The Division of Endocrinology, The Saban Research Institute, Children's Hospital Los Angeles, Los Angeles, California, USA[c]; Department of Molecular and Cellular Biology, Baylor College of Medicine, Houston, Texas, USA[d]; Institut de Génétique et de Biologie Moléculaire et Cellulaire, CNRS UMR7104/INSERM U964/Université de Strasbourg, Collège de France, Paris, France[e]; Department of Biochemistry and Molecular Biology, Keck School of Medicine, University of Southern California, Los Angeles, California, USA[f]

We previously showed that the orphan nuclear receptor Nur77 (Nr4a1) plays an important role in the regulation of glucose homeostasis and oxidative metabolism in skeletal muscle. Here, we show using both gain- and loss-of-function models that Nur77 is also a regulator of muscle growth in mice. Transgenic expression of Nur77 in skeletal muscle in mice led to increases in myofiber size. Conversely, mice with global or muscle-specific deficiency in Nur77 exhibited reduced muscle mass and myofiber size. In contrast to Nur77 deficiency, deletion of the highly related nuclear receptor NOR1 (Nr4a3) had minimal effect on muscle mass and myofiber size. We further show that Nur77 mediates its effects on muscle size by orchestrating transcriptional programs that favor muscle growth, including the induction of insulin-like growth factor 1 (IGF1), as well as concomitant downregulation of growth-inhibitory genes, including myostatin, Fbxo32 (MAFbx), and Trim63 (MuRF1). Nur77-mediated increase in IGF1 led to activation of the Akt-mTOR-S6K cascade and the inhibition of FoxO3a activity. The dependence of Nur77 on IGF1 was recapitulated in primary myoblasts, establishing this as a cell-autonomous effect. Collectively, our findings identify Nur77 as a novel regulator of myofiber size and a potential transcriptional link between cellular metabolism and muscle growth.

Skeletal muscle serves indelible roles in mediating locomotion and postural tone, as well as in the maintenance of energy homeostasis. Muscle wasting is commonly observed in patients with primary neuromuscular pathologies as well as in those with cancer cachexia. Much underappreciated, however, is the vast number of people who develop muscle atrophy as a comorbidity of aging, disuse, diabetes, heart failure, and chronic inflammatory illnesses. Muscle loss not only impairs the activities of daily living but also increases the risk of developing diabetes and of mortality (1–4). Current approaches of mitigating muscle loss—nutritional support and exercise—may be insufficient or infeasible in certain patient populations. Understanding the fundamental signaling pathways that control muscle mass is thus paramount to the development of novel therapies.

Maintenance of muscle mass in the adult animal depends largely on the balance of signals that favor growth or atrophy. Environmental cues, including protein excess, growth factors, physical exercise, and β-adrenergic stimulation, activate a complex array of overlapping signaling pathways affecting muscle homeostasis (5, 6). The most well known pathway, the insulin-like growth factor 1 (IGF1)–Akt–mTOR cascade, promotes protein synthesis through concurrent regulation of multiple components of the translational machinery. Muscle differentiation and growth are also modulated by mitogen-activated protein kinases (MAPKs) including extracellular signal-regulated kinase 1 and 2 (ERK1/2) and p38, which can be activated by calcium as well as calcium-independent pathways (7–11). PGC1α4 has also been shown to be a mediator of exercise-induced muscle hypertrophy (12).

On the other hand, conditions that induce muscle atrophy result in activation of the myostatin/transforming growth factor β (TGFβ) pathway. Myostatin and other TGFβ family members bind activin type II receptors, resulting in Smad2/3 phosphoryla-tion, increased forkhead box O (FoxO) protein activity, and a reduction in muscle mass (6, 13, 14). FoxO1 and FoxO3a are transcriptional regulators of the E3-ubiquitin ligases Fbxo32 (atrogin 1 or MAFbx) and Trim63 (MuRF1) that are upregulated upon muscle atrophy to degrade myofibrillar elements, MyoD, and components of the translation machinery. FoxO1 and FoxO3a are also negatively regulated by Akt-mediated phosphorylation, which retains these transcription factors in the cytoplasm (15). Because aspects of both protein synthesis and degradation are active during muscle remodeling (whether hypertrophy or atrophy), the balance of these complex and overlapping pathways ultimately determines the net effect on muscle mass.

The NR4A subfamily of nuclear receptors consists of three homologous members: Nur77 (NR4A1), Nurr1 (NR4A2), and NOR1 (NR4A3). These receptors are immediate early genes that possess ligand-independent activities. Their activities are primarily regulated at the transcriptional level as their expression is rapidly induced by cyclic AMP (cAMP), calcium, growth factors, and

stress ([16], [17]). In tissue-specific contexts, the three NR4A receptors can exhibit functional redundancy. We previously demonstrated that Nur77 is the most abundant NR4A isoform in skeletal muscle and that its expression is fast-twitch fiber selective. Furthermore, Nur77 is robustly induced by β-adrenergic stimulation and is dependent on innervation for maintenance of its expression ([18]). Studies from human subjects have revealed that Nur77 is among the genes most highly induced by strenuous cycling exercise ([19]). In this context, our identification of Nur77 as a regulator of glucose utilization genes in skeletal muscle suggests that Nur77 may be an important moderator of energy expenditure in exercise ([20]). We have also previously shown that muscle-specific overexpression of Nur77 increases mitochondrial DNA content, reduces mitochondrial fission, and increases oxidative metabolism ([21]). Interestingly, the muscle-specific NOR1 transgenic mouse also exhibits a striking increase in oxidative metabolism ([22]). These findings suggest that under conditions of sustained NR4A expression (such as in chronic stress), the NR4A receptors may alter the metabolic programming to increase energy efficiency by switching to oxidative metabolism.

In this study, we sought to identify functions of Nur77 in skeletal muscle by examining transcriptional programs altered by Nur77 overexpression in the MCK-Nur77 transgenic mouse. Unexpectedly, our results revealed that Nur77 induced the expression of a number of genes involved in muscle development and growth and altered myofiber size. Mice lacking Nur77 had correspondingly reduced myofiber size and muscle mass. These cellular changes were linked to the ability of Nur77 to orchestrate the transcriptional programs that support muscle growth, including the IGF1 pathway. Our results identify Nur77 as an important determinant of muscle mass and a potential transcriptional link between cellular metabolism and muscle growth.

MATERIALS AND METHODS

Microarrays. Total RNA was prepared from gastrocnemius muscle of overnight fasted mice by TRIzol (Life Technologies) extraction and purified through RNeasy columns (Qiagen). cRNA preparation and hybridization to Illumina MouseRef-6, version 2.0, arrays were performed by the Southern California Genotyping Consortium at UCLA. Six mice were used for each genotype. Data were analyzed using GeneSpring GX, version 10.0 (Agilent), and Ingenuity Pathway Analysis (IPA; Qiagen). Normalized intensity was generated after thresholding, log transformation, and normalization by GeneSpring's built-in algorithm. We included only genes with raw data signal greater than 100 for at least one condition for analysis.

Animal studies. The global Nur77$^{-/-}$ and MCK-Nur77 transgenic mice have been described previously ([18], [21]). The floxed Nur77 mouse (Nur77$^{flox/flox}$) was backcrossed to C57BL/6J mice for seven generations ([23]). The global NOR1$^{+/-}$ mouse was backcrossed to C57BL/6J mice for 10 generations ([24]). These two backcrossed strains were then mated to generate the compound mutant with Nur77$^{flox/flox}$/NOR1$^{+/-}$ genotype. Mice bearing the NOR1 mutant allele were mated as heterozygotes due to decreased fertility of the NOR1$^{-/-}$ mice. Finally, we bred the MCK-Cre mouse (on a mixed C57BL/6J and C57BL/6N background) (catalog number 006475; The Jackson Laboratory) to the compound mutant to generate control (Cre$^-$/Nur77$^{flox/flox}$/NOR1$^{+/+}$), muscle-specific Nur77-null (mNur77$^{-/-}$ mice; Cre$^+$/Nur77$^{flox/flox}$/NOR1$^{+/+}$), single global NOR1-null (Cre$^-$/Nur77$^{flox/flox}$/NOR1$^{-/-}$), and compound deletion of muscle Nur77 and NOR1 (mDKO, for muscle double-knockout, mice; Cre$^+$/Nur77$^{flox/flox}$/NOR1$^{-/-}$) mice. We used the following primers for genotyping: Nur77$^{flox/flox}$ forward, 5′ AGG ACA CCC ATG CTC ATG TG 3′, and reverse, 5′ TGA CAC CCT CAC ACG GAC AA 3′ (wild type, 200-bp

amplicon; Nur77^{flox}, 300-bp amplicon); MCK-Cre forward, 5′ ATG TCC AAT TTA CTG ACC G 3′, and reverse, 5′ CGC GCC TGA AGA TAT AGA AG 3′ (Cre$^+$, 350-bp amplicon; Cre$^-$, no amplification). Genotyping primers for NOR1$^{-/-}$ were reported elsewhere ([25]). Mice were fed *ad libitum* and maintained on a 12-h light-dark cycle and were age and gender matched for all experiments. Body composition was measured using the EchoMRI Analyzer (EchoMRI LLC). Animal studies were performed in accordance with University of California at Los Angeles (UCLA) Animal Research Committee guidelines.

Cell lines and treatment. Primary murine myoblasts were isolated from neonatal pups (<7 days old) as previously described ([26]). Myoblasts were cultured in 20% fetal bovine serum (FBS)–F-10 medium with basic fibroblast growth factor (bFGF) supplementation at 2.5 ng/ml (PHG0021; Life Technologies) and seeded on extracellular matrix (ECM) (E1270; Sigma) according to the manufacturer's instructions. At confluence, medium was switched to 5% horse serum in Dulbecco's modified Eagle's medium (DMEM) to initiate differentiation. Differentiation medium was refreshed daily. For adenoviral infections, cells were transduced overnight with adenovirus-green fluorescent protein (Ad-GFP) or Nur77 at a multiplicity of infection (MOI) of 200 with 10 μg/ml Polybrene in 5% FBS-DMEM. Total RNA was prepared by TRIzol 48 h after transduction.

Immunostaining of cryosections. Muscle was flash frozen in liquid nitrogen-chilled isopentane. Frozen sections (10 μm) were air dried for 5 min and then fixed by 4% paraformaldehyde-PBS (for type 2d fibers) or ice-cold 4% acetone-phosphate buffered saline (PBS) (for all other fiber types). Sections were quenched, permeabilized, and blocked as previously described ([27]). Primary antibodies were purchased from the Developmental Studies Hybridoma Bank (type 1 fiber, A4.84; type 2a fiber, SC-71; type 2b fiber, BF-F3; and type 2d fiber, 6H1) and Sigma (laminin; L9393). Secondary antibodies used were goat anti-mouse IgM–fluorescein isothiocyanate (FITC) (type 1, 2b, and 2d) and goat anti-mouse IgG–Alexa Fluor 555 (type 2a) from Southern Biotechnology and goat anti-rabbit IgG–Alexa Fluor 350 (laminin) from Life Technologies. Stained sections were imaged with Zeiss Axio Skop 2 Plus and Axio Observer inverted fluorescence microscopes and a color charge-coupled-device (CCD) camera. Fiber cross-sectional area was determined by Fiji. We used between 4 and 11 mice of each genotype to determine fiber size.

Analysis of primary myotube differentiation. Primary myoblasts were seeded on ECM-coated chamber slides (80826; Ibidi) and differentiated at confluence as described above. R3 IGF1 (50 ng/ml) (I1146; Sigma) or 100 nM BMS-754807 (S1124; Selleckchem) was included in the differentiation medium for a total of 4 days. Fixation and staining were performed as described previously ([28]). Cells were incubated with anti-sarcomeric myosin heavy chain (MF20; Developmental Studies Hybridoma Bank) overnight at 4°C, followed by incubation with Alexa Fluor 488-conjugated secondary antibody for 1 h at room temperature. Cells were stained with 4′,6′-diamidino-2-phenylindole (DAPI) solution for 5 min and then mounted with Ibidi mounting medium (50001; Ibidi). Cells were imaged as above. Image analysis was done using Fiji. Myotube diameter was averaged from three measurements across the length of each myotube. A total of 100 myotubes were counted for each condition. Fusion efficiency was calculated as the percentage of nuclei found within MF20-immunoreactive cells out of the total number of nuclei in 8 to 10 fields imaged at a magnification of ×5.

RNA and protein analysis. Total RNA preparation and quantitative real-time PCR were performed as described previously ([18]). Expression was normalized to 36B4 expression. Primer sequences are listed in Table S1 in the supplemental material and are as previously described ([18]). Frozen muscle tissue was homogenized in radioimmunoprecipitation assay (RIPA) buffer (with 1 mM phenylmethylsulfonyl fluoride [PMSF], 1× Complete protease inhibitor and PhosSTOP inhibitor from Roche) with a motorized Teflon pestle. Sources of antibody and dilutions are as follows: from Cell Signaling Technology, phospho-Akt (p-Akt) (S473) at 1:1,000 (product number 4058), Akt at 1:5,000 (9272), p-mTOR (S2448) at 1:1,000 (5536), mTOR at 1:2,000 (2983), p-P70S6K (Thr389) at 1:1,000

TABLE 1 Top pathways (diseases and biological functions) differentially regulated by Nur77

Pathway and function	P value	No. of genes
Diseases and disorders		
Neurological disease	4.44E−08 to 2.02E−02	98
Skeletal and muscular disorders	1.33E−05 to 2.02E−02	85
Hereditary disorder	1.41E−05 to 2.02E−02	67
Psychological disorders	1.41E−05 to 2.02E−02	64
Cardiovascular disease	3.33E−05 to 2.02E−02	62
Molecular and cellular functions		
Cellular assembly and organization	1.55E−04 to 2.02E−02	43
Lipid metabolism	1.55E−04 to 2.02E−02	34
Molecular transport	1.55E−04 to 2.02E−02	76
Small molecule biochemistry	1.55E−04 to 2.02E−02	48
Cell morphology	2.68E−04 to 2.02E−02	50
Physiological system development and function		
Embryonic development	2.09E−04 to 2.02E−02	29
Organ development	2.09E−04 to 2.02E−02	21
Organismal development	2.09E−04 to 2.02E−02	27
Tissue development	2.09E−04 to 2.02E−02	41
Visual system development and function	2.09E−04 to 1.05E−02	8

(9205), P70S6K at 1:2,000 (9202), p-S6 (S235) at 1:2,000 (4858), histone deacetylase 4 (HDAC4) at 1:1,000 (5392), HDAC5 at 1:1,000 (2082), p-Smad2 (S465/467) at 1:1,000 (3108), p-Smad3 (S423/425) at 1:1,000 (9520), Smad2/3 at 1:1,000 (9523), FoxO1 at 1:1,000 (2880), FoxO3a at 1:1,000 (2497), p-FoxO1 (Thr24)/FoxO3a (Thr32) at 1:1,000 (9464), p-p42/44 MAPK (Thr202/Tyr204) at 1:1,000 (4376), p42/44 MAPK at 1:1,000 (9102), p-p38 MAPK (Thr180/Tyr182) at 1:1,000 (9211), and p38 MAPK at 1:1,000 (9212); from GeneTex, P84 at 1:5,000 (GTX70220); from Abcam, p-HDAC4 (S632) at 1:1,000 (ab39408) and p-HDAC5 (S259) at 1:1,000 (ab53693). Antibody binding was detected by ECL Plus (Pierce), using ImageQuant LAS4000 (GE) for image capture. Fiji was used for quantification of band intensity.

Statistical analysis. A Student t test was used to determine statistical significance. Error bars represent standard errors of the means unless otherwise noted. Statistical significance between mean fiber sizes was determined using an unpaired t test with Welch's correction.

Microarray data accession number. Microarray data are available from GEO DataSets under accession number GSE65585.

RESULTS

Differential expression of muscle development and growth genes in skeletal muscle of Nur77-overexpressing mice. We previously showed that Nur77 is a transcriptional regulator of glucose metabolism in skeletal muscle (18, 20). Subsequent studies of muscle-specific Nur77 and NOR1 transgenic mouse models demonstrated a role for these receptors in augmenting mitochondrial respiration and oxidative metabolism in skeletal muscle (21, 22, 29). To reveal additional functions of Nur77 in skeletal muscle, we performed expression profiling of total muscle RNA from wild-type and MCK-Nur77 transgenic mice. Our analysis identified over 500 genes whose expression was either up- or downregulated at least 2-fold by Nur77 expression (see Table S2 in the supplemental material). We next performed network/functional analysis of this subset of genes using Ingenuity Pathway Analysis (IPA; Qiagen). In this unbiased ranking, the most highly regulated genes in the diseases and disorders category were associated with neurological disease, followed by genes linked to skeletal and muscular disorders (Table 1). Further examination of the 85 genes in the latter group pointed to multiple genes involved in muscle development and growth (Table 2). Specifically, Nur77 increased the expression of insulin-like growth factor 1 (IGF1), a well-established myogenic factor, as well as a number of developmental myosin genes, including those for Myh3, Myh8, and Myl4. Concomitantly, Nur77 downregulated the expression of the atrogenes encoding Trim63 (MuRF1) and Fbxo32 (atrogin1 or MAFbx), two E3 ligases induced in the setting of muscle atrophy. This constellation of gene expression changes implicated Nur77 as a potential regulator of muscle growth and development.

Nur77 overexpression increases myofiber size in transgenic mice. The gene expression profile of the MCK-Nur77 transgenic muscle prompted us to explore whether Nur77 expression had an impact on muscle mass or myofiber size. As shown in Fig. 1A to D, Nur77 transgenic and littermate control mice have comparable body masses and gastrocnemius masses, as well as lean body mass, although the gastrocnemius muscle mass was slightly reduced

TABLE 2 Nur77 regulation of genes involved in muscle development and growth

| Symbol	Gene name	GenBank accession no.	Fold change (TG/WT)[a]	P value
MYH8	Myosin, heavy chain 8, skeletal muscle, perinatal	NM_177369.3	107.5	1.99E−05
MYH3	Myosin, heavy chain 3, skeletal muscle, embryonic	XM_354614.1	16.3	0.00178
MYL4	Myosin, light chain 4, alkali; atrial, embryonic	NM_010858.3	3.9	0.00152
ACTC1	Actin, alpha, cardiac muscle 1	NM_009608.1	3.1	0.00152
MAMSTR	MEF2-activating motif and SAP domain-containing transcriptional regulator	NM_172418.1	3.1	1.82E−05
CHRNB1	Cholinergic receptor, nicotinic, beta 1 (muscle)	NM_009601.3	2.3	7.52E−04
FHL1	Four and a half LIM domains 1	NM_001077362.1	2.3	3.43E−05
CHRNA1	Cholinergic receptor, nicotinic, alpha 1 (muscle)	NM_007389.2	2.1	0.00266
IGF1	Insulin-like growth factor 1 (somatomedin C)	NM_010512.2	2.1	0.0089
CAMK2A	Calcium/calmodulin-dependent protein kinase II alpha	NM_177407.2	−2.0	3.31E−04
MUSK	Muscle, skeletal, receptor tyrosine kinase	NM_001037129.1	−2.8	0.00457
FBXO32	F-box protein 32	NM_026346.1	−3.1	0.00490
Trim63	Tripartite motif containing 63, E3 ubiquitin protein ligase	NM_001039048.2	−3.5	0.00280
IGFALS	Insulin-like growth factor binding protein, acid labile subunit	NM_008340.2	−5.3	2.27E−05

[a] TG, transgenic; WT, wild type.
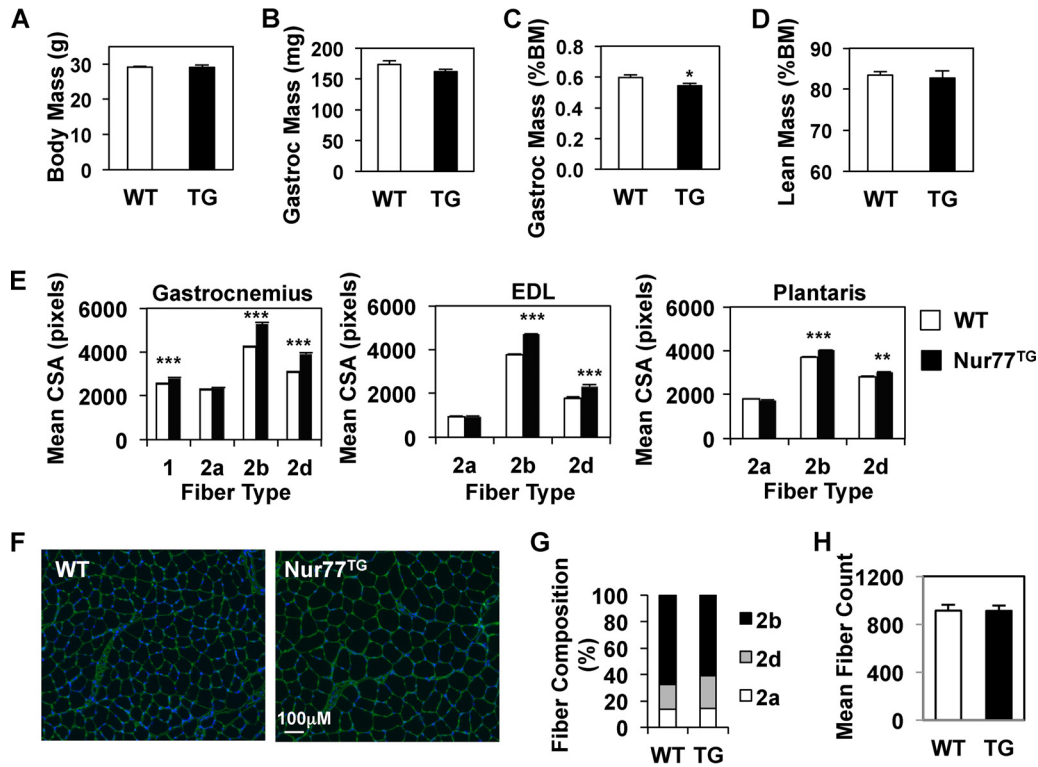
FIG 1 Morphometric analysis and myofiber size of MCK-Nur77 transgenic mice. Body mass (BM) (A), absolute (B) and relative (C) gastrocnemius mass of wild-type (WT) and Nur77-transgenic (TG) mice, and lean mass of 6- to 8-month-old male mice measured by EchoMRI ($n = 7$) (D) were determined. (E) Mean cross-sectional area (CSA) of myofibers from the red gastrocnemius, EDL, and plantaris muscles. (F) Representative immunofluorescence images from wild-type and transgenic gastrocnemius cross sections at a magnification of ×10. The cell border is outlined by antilaminin antibody (green). Nuclei were detected by DAPI staining. (G and H) Fiber composition and mean fiber count of EDL muscle. Four to six female mice were used per genotype. For panels A to C, E, and F, $n = 5$ or 6 male, 4-month-old mice; for panels G and H, $n = 4$ to 6 female, 5-month-old mice. *, $P < 0.05$; **, $P < 0.01$; ***, $P < 0.001$.

when corrected for body mass. At the level of muscle fibers, however, the mean cross-sectional area of slow-twitch type 1 and fast-twitch type 2b and 2d fibers but not fast-twitch oxidative type 2a fibers was significantly larger in the Nur77-overexpressing gastrocnemius muscle (Fig. 1E and F). We observed similar fiber size increases for type 2b and 2d fibers of the transgenic extensor digitorum longus (EDL) and plantaris muscles (Fig. 1E). There was a trend toward an increase in the abundance of type 2d fibers at the expense of type 2b fibers in the EDL muscle from transgenic mice although the difference did not reach statistical significance (Fig. 1G). Since Nur77 overexpression did not increase the overall muscle mass, we reasoned that the increase in myofiber cross-sectional area must be accompanied by a concordant reduction in fiber count. Although we did not observe a statistically significant difference in the total number of fibers in EDL by counting (Fig. 1H), we cannot exclude the possibility of a subtle difference, given the limitation of the approach. We also cannot exclude the possibility that there is an adaptive reduction in fiber numbers in other muscle groups in Nur77-overexpressing mice as it is difficult to determine fiber numbers by cross-sectional analysis in nonlongitudinal muscles such as the gastrocnemius.

Genetic deletion of Nur77 reduces muscle mass. Having shown that Nur77 overexpression increases myofiber size, we next investigated if Nur77 deletion would result in the opposite phenotype. To test this hypothesis, we examined the muscles of the global Nur77-deficient mouse. As shown in Fig. 2A to E, global

Nur77$^{-/-}$ mice had reduced body mass as well as tibialis anterior (TA) and gastrocnemius mass. To address the potential confounding effect of Nur77 deletion in nonmuscle tissues, we generated a muscle-specific Nur77-null mouse (mNur77$^{-/-}$) by introducing the MCK-Cre recombinase allele into the homozygous Nur77$^{flox/flox}$ mouse (23). Prior work has shown that the three members of the NR4A family regulate many of the same target genes and that the expression of NOR1 is increased in the genetic absence of Nur77 (18, 22, 29, 30). We therefore also assessed the possible contribution of NOR1 to muscle size by crossing the global NOR1$^{-/-}$ mouse (24) onto the MCK-Cre$^+$/Nur77$^{flox/flox}$ background (abbreviated as mDKO for muscle double knockout). Due to the lack of commercial antibodies that can detect Nur77 protein in muscle lysates with specificity, we verified Cre-mediated deletion of Nur77 by measuring the expression of Nur77 and its target Fbp2 gene by quantitative real-time PCR. As shown in Fig. 3A, loss of Nur77 in the mNur77$^{-/-}$ and mDKO mice resulted in a 10-fold reduction in the expression of Nur77 transcript and a 5-fold reduction in the canonical Nur77 target Fbp2 gene. These findings confirmed effective deletion of the floxed Nur77 allele by the Cre recombinase in skeletal muscle.

We next conducted morphometric analysis on both male and female mice. Male mNur77$^{-/-}$ mice exhibited reduced body mass (BM), as well as a reduction in absolute and relative tibialis anterior (TA) and gastrocnemius muscle mass (Fig. 3B to F). A reduction in muscle mass of 11% and 13% was seen in the TA and
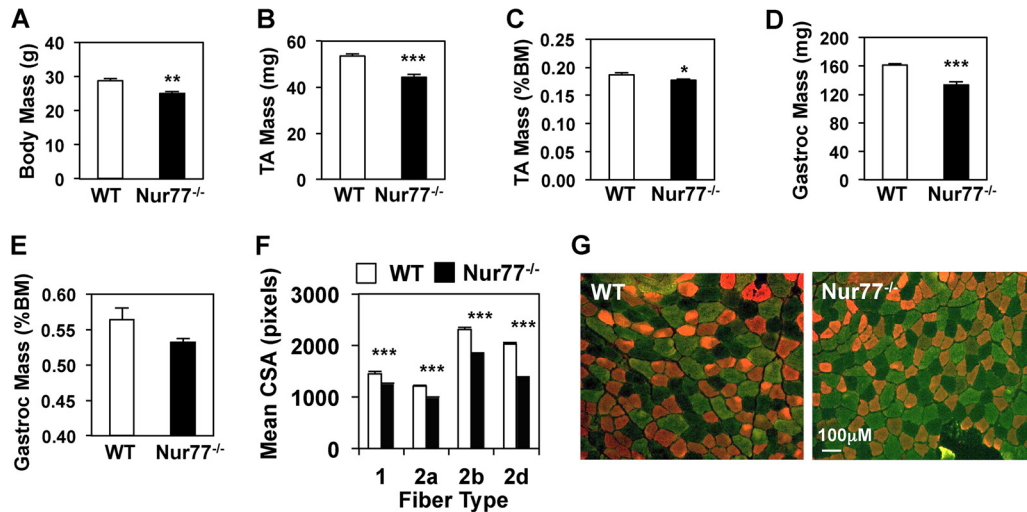
FIG 2 Nur77-deficient mice have reduced muscle mass. Body mass (A) and absolute (B and D) and relative (C and E) mass of tibialis anterior (TA) and gastrocnemius (gastroc) muscles of 4-month-old male wild-type (WT) and global Nur77 knockout (Nur77$^{-/-}$) mice were determined. (F) Mean cross-sectional area (CSA) of muscle fibers from the red gastrocnemius muscle. (G) Representative immunofluorescent staining of type 2b (green) and 2a (red) fibers of wild-type and Nur77$^{-/-}$ gastrocnemius cross sections at a magnification of ×10. *, $P < 0.05$; **, $P < 0.01$; ***, $P < 0.001$ ($n = 6$ to 7).

gastrocnemius muscle, respectively, in mice with muscle-specific deletion of Nur77. Deletion of NOR1 alone did not alter muscle mass. Nur77-mediated reduction in muscle mass was supported by lean mass measurement obtained by EchoMRI (Fig. 3M). Compared to mNur77$^{-/-}$ mice, compound deletion of Nur77 and NOR1 further reduced the relative mass of TA (13% versus 21%, $P = 0.025$) but not that of gastrocnemius. We observed a similar synergistic effect of Nur77 and NOR1 deletion on TA (19% versus 9%; $P = 0.004$) but not gastrocnemius muscle in female mice (Fig. 3G to K). Thus, using two independent mouse models of Nur77 deletion, we have demonstrated that loss of Nur77 compromises adult muscle mass. Furthermore, it is clear that these effects are due to the intrinsic action of Nur77 signaling in muscle.

The reduction of muscle mass of global Nur77 knockout mice correlated with a shift toward smaller myofibers in all four fiber types of the gastrocnemius muscle (Fig. 2F to G). The mean cross-sectional area of the muscle-specific Nur77-null mice was similarly concordant with the changes in muscle mass in this model (Fig. 3L) (for type 2b fibers, in flox/flox mice, 1,535 ± 12; mNur77$^{-/-}$, 1,344 ± 8; NOR1$^{-/-}$, 1,466 ± 12; mDKO, 1,177 ± 7 pixels; $P < 0.0001$ for all t test comparisons). Compared to Nur77$^{flox/flox}$ controls, mice with muscle Nur77 deletion alone (mNur77$^{-/-}$) exhibited a 12.4% reduction in mean cross-sectional area. NOR1 deletion had a small but statistically significant effect on fiber size (4.5% reduction). Compound deletion of both muscle Nur77 and global NOR1 profoundly reduced the mean fiber size by 23.3%. These findings support partial functional redundancy between Nur77 and NOR1, with Nur77 playing the dominant role in the control of muscle mass.

Nur77 regulates the expression of growth-promoting and growth-limiting genes in muscle. We next sought to determine if the changes in myofiber size in our Nur77 gain- and loss-of-function models could be explained by changes in the expression of genes linked to muscle growth regulation. In the MCK-Nur77 transgenic mice, we confirmed an approximately 5-fold increase in Nur77 expression by quantitative reverse transcription-PCR

(qRT-PCR) (Fig. 4) (21). As shown in Table 2, microarray analysis of global gene expression in muscle of MCK-Nur77 transgenic mice revealed robust upregulation of IGF1, an integral growth factor that controls muscle development, postnatal muscle hypertrophy, and muscle regeneration (31–33). We validated this finding with qRT-PCR (Fig. 4) and then extended our analysis to examine other growth-related genes. Nur77-overexpressing muscle exhibited an increase in expression of other growth-promoting genes as well, including those for IGF2 and eukaryotic translation initiation factor 4A1 (eIF4A1). We also observed marked upregulation of Dachshund 2 (Dach2), a previously identified activator of myogenesis (34) (Fig. 4).

We next measured the expression of growth-limiting genes. The expression of histone deacetylases 4 and 5 (HDAC4 and HDAC5, respectively, or HDAC4/5), which act as repressors of myogenic genes, including the MEF2 and Dach2 genes, trended lower in Nur77-overexpressing muscle (Fig. 5). Confirming our microarray findings (Table 2), transgenic muscle had reduced expression of the E3 ligases Trim63 (MuRF1) and Fbxo32 (MAFbx) (Fig. 4). Deletion of these genes is muscle sparing under certain atrophy-inducing conditions (35–37). In addition, the expression of myostatin (Mstn) (a negative regulator of muscle mass) and TWEAK receptor (Tnfrsf12a) (also implicated in muscle atrophy) was downregulated in Nur77 transgenic muscle (Fig. 4) (38, 39). The expression Fbxo40, an E3 ligase that limits IGF signaling by degrading IRS1, also trended lower in MCK-Nur77 muscle (40, 41). On balance, our results reveal that Nur77 expression in skeletal muscle directs a transcriptional program that supports myogenesis and protein synthesis. Nur77 simultaneously represses genes normally induced in muscle atrophy to support fiber hypertrophy.

We next examined the expression of growth-regulating genes in global Nur77-deficient mice. As expected, Nur77 gene deletion abolished Nur77 mRNA expression (Fig. 5). Among the growth-promoting genes, we observed significant downregulation of IGF1 and eIF4A1 and a trend for reduced IGF2 expression in Nur77-null muscle. Dach2 expression was unchanged. Among the
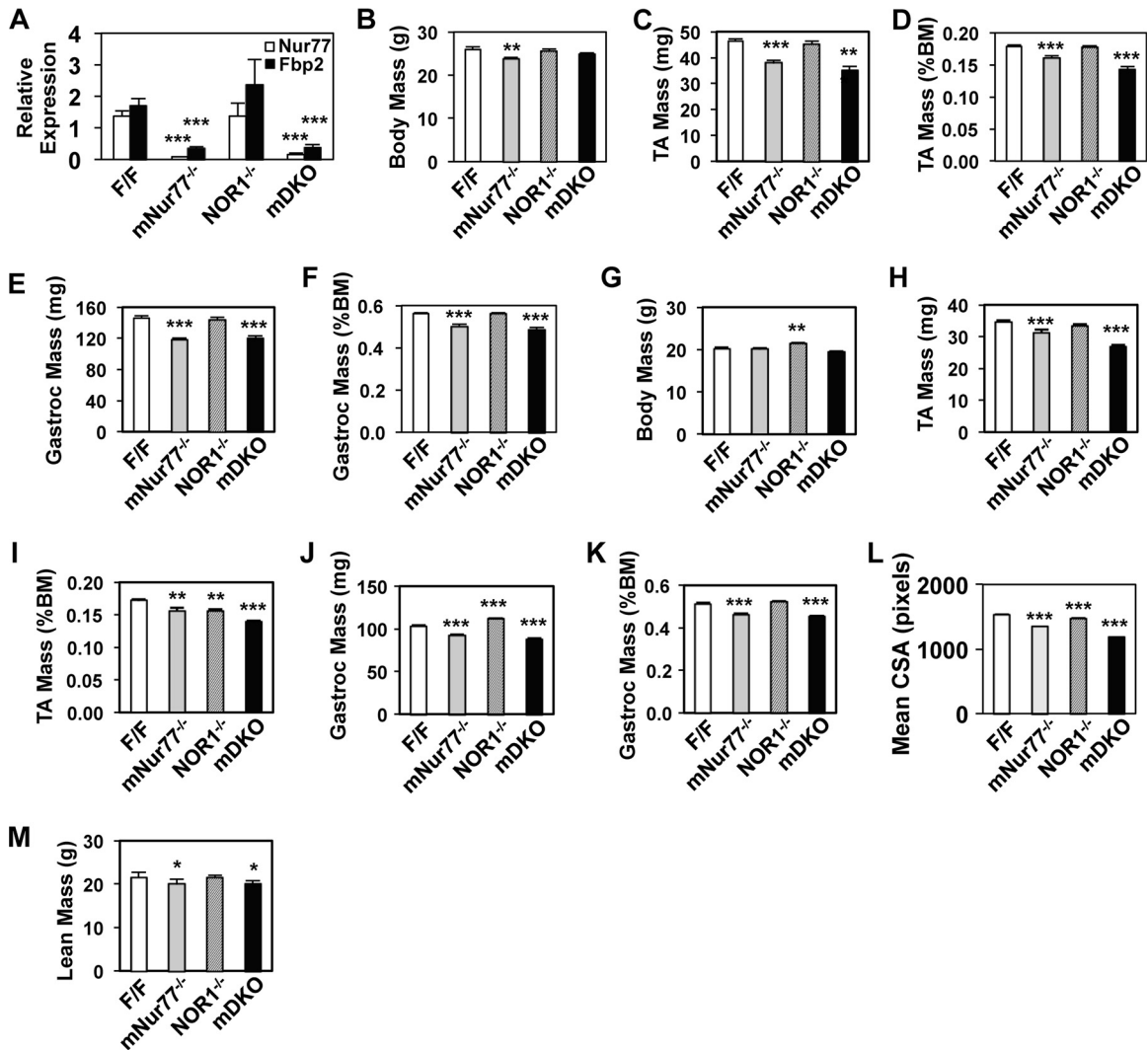
FIG 3 Muscle-specific deletion of Nur77 is sufficient to reduce muscle size. (A) Nur77 deletion in mNur77$^{-/-}$ and mDKO muscle abolished Nur77 and Fbp2 expression. Body mass and muscle mass of male (B to F) and female (G to K) control (flox/flox [F/F]), muscle-specific Nur77$^{-/-}$ (mNur77$^{-/-}$), global NOR1$^{-/-}$, and muscle-specific Nur77$^{-/-}$/global NOR1$^{-/-}$ (mDKO) mice were determined. (L) Mean cross-sectional area of type 2b fibers of the extensor digitorum longus muscle. (M) Lean mass of male mice determined by EchoMRI. Comparison is between the floxed control and other genotypes. **, $P < 0.01$; ***, $P < 0.001$. For panels A and L, $n = 5$ or 6; for panel M, $n = 6$ to 8; for all other panels, $n = 8$ to 11.

growth-limiting genes, we observed a small but statistically significant increase in the expression of HDAC4, Trim63, and Fbxo32 (Fig. 5). HDAC5 and Mstn expression levels were unchanged by Nur77 deletion. Overall, these changes in expression of growth-regulating genes are consistent with the observation of muscle hypotrophy in Nur77-null mice. Taking into consideration the changes in growth-regulating genes in both Nur77-overexpressing and Nur77-deficient muscle, we propose that Nur77 controls muscle mass by upregulating IGF1 and eIF4A1 while suppressing the expression of a battery of genes that limit muscle growth.

To determine if the changes in gene expression in the MCK-Nur77 transgenic mouse reflect proximal effects of Nur77 expression or rather chronic adaptive responses, we examined the effect of acute Nur77 expression on gene expression in primary murine myotubes. As shown in Fig. 6A, adenovirus-mediated overexpression of Nur77 led to induction of IGF1 and eIF4A1 and repression of Mstn and Trim63, recapitulating our in vivo observations. Un-

expectedly, whereas IGF2 expression was robustly induced in transgenic muscle in vivo, the expression of IGF2 in primary myotubes was suppressed. This discrepancy could reflect loss of certain feedback regulation from the heterogeneous milieu of skeletal muscle. We also noted that adenoviral Nur77 expression increased, rather than decreased, the expression of Fbxo32. We observed a similar pattern of regulation in C2C12 myotubes overexpressing Nur77 (data not shown). It was previously shown that muscle Fbxo32 is expressed at higher levels in Trim63-null mice than in control mice after denervation (42). This suggests that Trim63 may be a negative regulator of Fbxo32 in certain biological contexts (for instance, in Trim63-deficient muscle or in cultured myotubes). Overall, the changes in Nur77-mediated gene expression in primary myotubes support the hypothesis that Nur77 controls muscle mass by orchestrating a transcriptional programming of growth-regulating genes.

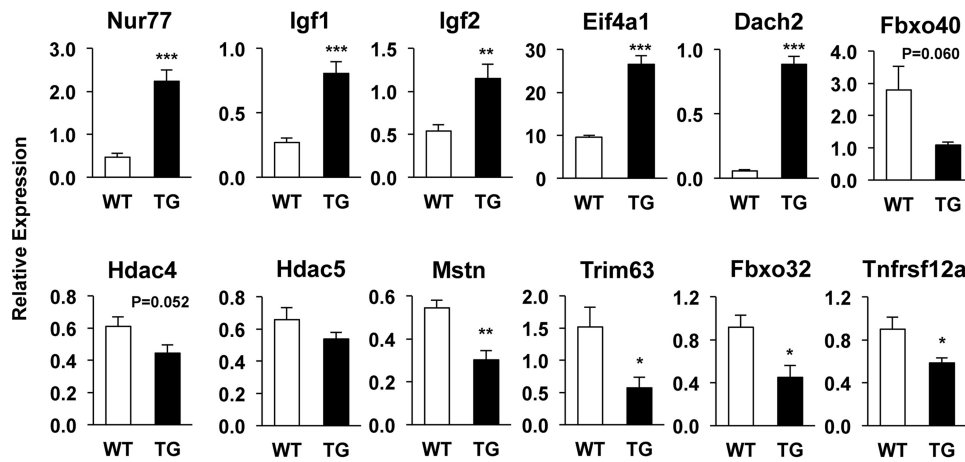Based on the gene expression data above, we performed in silico

FIG 4 Gene expression analysis of Nur77-overexpressing transgenic muscle. Expression of growth-regulating genes in white quadriceps muscle of 4-month-old male mice. Expression was analyzed by quantitative real-time PCR and normalized to 36B4 control ($n = 7$ to 9). *, $P < 0.05$; **, $P < 0.01$; ***, $P < 0.001$.

analysis of the genes positively regulated by Nur77 to identify putative Nur77-binding response elements (NBRE) (43). Near the mouse IGF2 locus, the consensus Nur77-binding sequence AAAGGTCA was present at 12,389 bp, 15,068 bp, and 15,209 bp downstream of the 3′ untranslated region (UTR) although these sites were not conserved in human. A nonconserved consensus sequence was also identified 7,298 bp downstream of the eIF4A1 3′ UTR. A similar analysis done on the IGF1 gene revealed 10 putative Nur77 binding sites within 10 kb of the gene. As shown in Fig. 6B, the site located in intron 3 is conserved across mouse, rat, and human, suggesting that this may be the site mediating Nur77 regulation of IGF1.

IGF1-dependent growth of mutant Nur77 myoblasts. To further determine the importance of IGF1 in Nur77-mediated control of myofiber growth, we examined the differentiation of Nur77 mutant myoblasts with and without IGF1. Recapitulating our *in vivo* findings, primary myoblasts isolated from global Nur77-deficient mice demonstrated impaired differentiation, with the formation of fewer, shorter, and smaller myotubes (Fig. 6C to E). IGF1 was able to augment the diameter of Nur77-deficient myo-

tubes, although the recovery was not to the level of wild-type myotubes. In our hands, the presence of IGF1 did not significantly alter the differentiation index of the myoblasts. We observed similar findings from primary myoblasts isolated from muscle-specific Nur77-null mice (data not shown). Conversely, primary myoblasts from MCK-Nur77 transgenic mice formed larger myotubes than those of wild-type cells (Fig. 6F). Inhibition of IGF1 signaling with the IGF-1R inhibitor BMS-754807 (44) diminished the diameter of both wild-type and transgenic myotubes although the latter remained slightly larger than those of the wild-type controls. Nur77 overexpression did not affect the differentiation index (Fig. 6G). These findings are consistent with a model in which Nur77 regulates local IGF1 expression to direct muscle growth in a cell-autonomous fashion. Since manipulating IGF1 did not fully restore the myotube size of mutant Nur77 cells, we conclude that Nur77 likely exerts both IGF1-dependent and -independent effects on muscle growth.

Nur77 modulates Akt-S6K, Smad2/3, and FoxO3 signaling. The hypertrophic effect of IGF1 is largely mediated by signaling
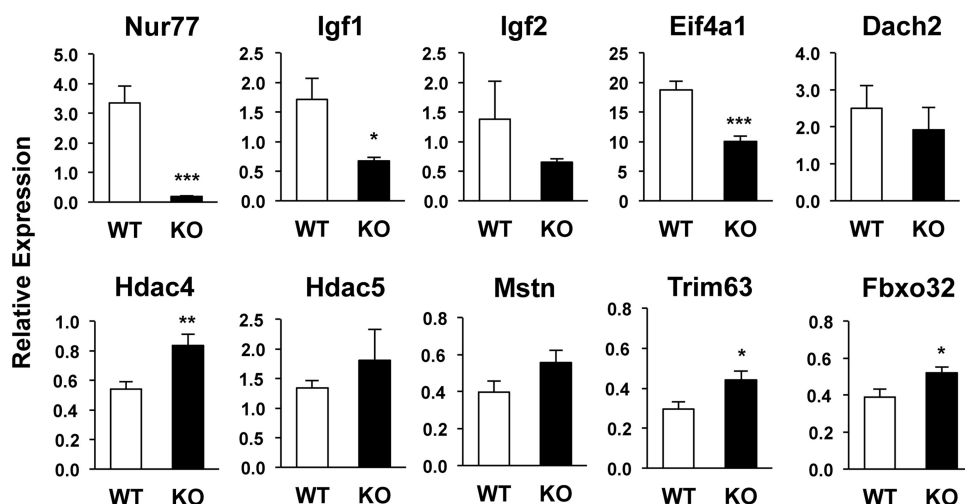

FIG 5 Gene expression analysis of global Nur77$^{-/-}$ muscle. Expression of growth-regulating genes in white quadriceps muscle of 4-month-old male mice ($n = 6$). *, $P < 0.05$; **, $P < 0.01$; ***, $P < 0.001$.
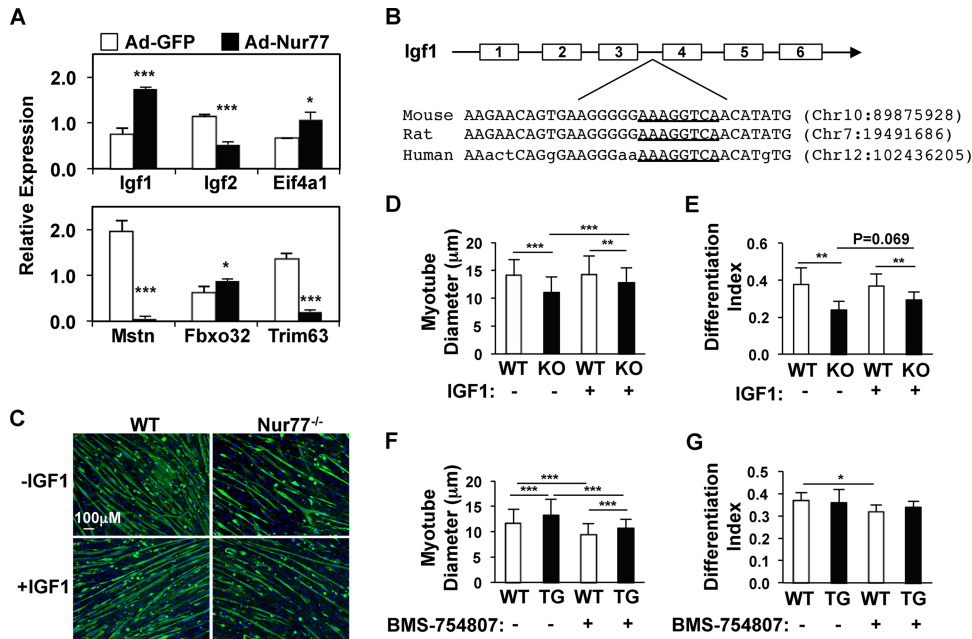
FIG 6 Nur77 regulation of myotube differentiation and size is mediated by IGF1. (A) Gene expression analysis of primary myotubes transduced with adenoviral (Ad) Nur77 for 48 h. Expression was analyzed by quantitative real-time PCR and normalized to the 36B4 control. Results are representative of three independent experiments ($n = 3$ per condition). (B) Schematic of the mouse IGF1 locus (not drawn to scale) and alignment of the conserved NBRE (underlined) is shown. Nonconserved nucleotides are shown in lowercase letters. (C to E) IGF1 rescue of the reduced myotube diameter observed in Nur77-deficient primary myoblasts. Green fluorescence represents differentiated myoblasts, and nuclei are marked by DAPI (blue) (C). (F and G) Inhibition of IGF1 receptor with BMS-754807 partially attenuated the effect of Nur77 overexpression on myotube diameter. Error bars indicate standard deviations. *, $P < 0.05$; **, $P < 0.01$; ***, $P < 0.001$. WT, wild-type; KO, Nur77 knockout; TG, transgenic.

through the Akt-mTOR-S6K cascade. In addition, this pathway engages in cross talk with FoxO and the signaling cascade downstream of myostatin to support a cellular program that tips the balance toward protein synthesis and away from proteolysis. Based on our observation that Nur77 regulates IGF1 expression, we sought to determine if these pathways were altered in response to changes in Nur77 activity. Indeed, in MCK-Nur77 transgenic muscle lysates, we observed increased phosphorylation of Akt (Ser473) and of P70S6K (Thr389) and its substrate S6 (Ser235), which collectively would be expected to promote protein synthesis and muscle growth (Fig. 7). To our surprise, mTOR phosphorylation was unchanged, suggesting that activation of P70S6K and its downstream target S6 may be the result of other signaling inputs, such as through the Gai2-protein kinase C (PKC) pathway (6). In addition to the Akt-mTOR pathway, we also examined several other protein kinases implicated in IGF1-mediated signaling, including p38 and p42/p44 MAPKs. In Nur77 transgenic lysates, we observed decreased p38 phosphorylation, which may contribute to the downregulation of Fbxo32 (45). On the other hand, Nur77 overexpression led to increased phosphorylation of p42 (but not p44) MAPK, which has been shown to be an important factor in protein translation and terminal differentiation of myoblasts (46–48).

Based on the role of HDAC4 and HDAC5 in myogenesis and muscle hypertrophy, we next measured the effect of Nur77 on the phosphorylation state of these cosuppressors. The activity of HDAC4/5 is dependent on its localization, wherein CaMK-mediated phosphorylation triggers nuclear export and relief of their repressive effect on MEF2 activity (49–51). It was thus unexpected that transgenic muscle lysate exhibited a trend toward increased

total HDAC4 protein and a statistically significant reduction in p-HDAC4 (Ser632) (Fig. 7). This finding would increase the abundance of active HDAC4 to exert a growth-limiting effect. Phosphorylation of HDAC5 was unaffected in Nur77 transgenic mice. Since HDAC4 is phosphorylated by many kinases besides CaMK, we speculate that the reduction in p-HDAC4 may relate to changes in other kinases, which may serve to limit the effect of hypertrophic signaling.

Nur77-mediated downregulation of genes such as those for myostatin, Trim63, and Fbxo32 led us to next examine signaling changes involved in muscle atrophy. Myostatin binding to the activin receptor II receptors leads to phosphorylation of Smad2/3 and its inhibition of Akt (6, 52). In Nur77 transgenic muscle lysates, we observed a small but statistically significant reduction in Smad2 phosphorylation at Ser465/467 (Fig. 7). Phosphorylation of Smad3 at Ser423/425 (as a percentage of total Smad3) was unchanged although the total Smad3 level tended to decrease in transgenic lysate. Overall, these findings suggest reduced myostatin-mediated signaling, consistent with a decrease in myostatin mRNA level. The expression of the atrogenes encoding Trim63 and Fbxo32 is largely controlled by the activity of the FoxO transcription factors, which are negatively regulated by Akt phosphorylation and nuclear exclusion. As shown in Fig. 7, whereas FoxO1 phosphorylation was unchanged ($P = 0.11$), FoxO3a phosphorylation was increased in Nur77 transgenic lysates, consistent with diminished FoxO3a transcriptional activity and downregulation of atrogenes (45).

Overall, Nur77 overexpression in skeletal muscle resulted in increased Akt/S6K, p42 MAPK, and FoxO3a signaling but reduced
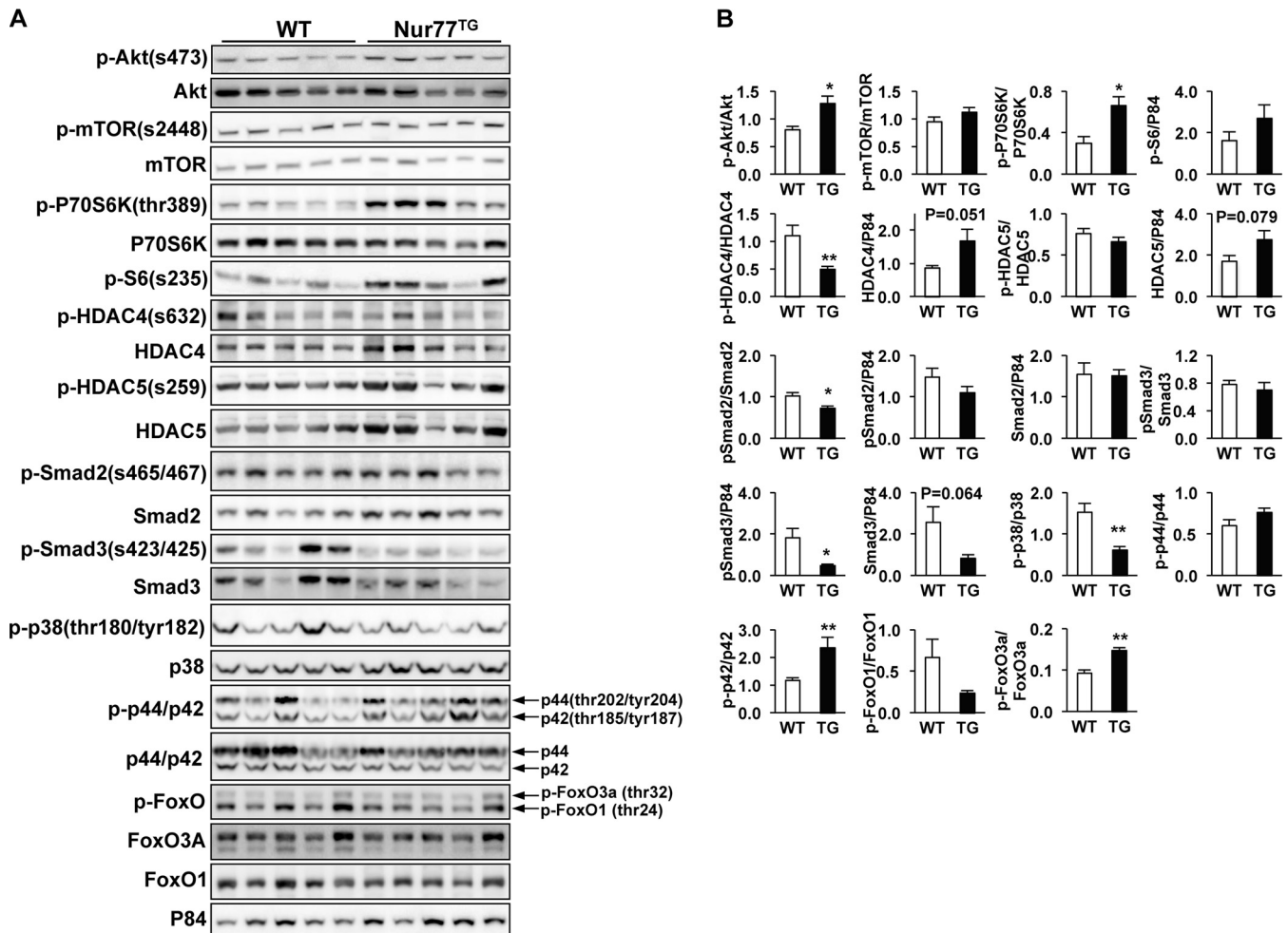
FIG 7 MCK-Nur77 transgenic muscle exhibited increased Akt-S6K and FoxO3a signaling and diminished Smad2/3 signaling. (A) Immunoblot analysis of total lysates prepared from white quadriceps muscle of Nur77 transgenic mice. (B) Densitometry quantification of the results from panel A. *, $P < 0.05$; **, $P < 0.01$; ***, $P < 0.001$ ($n = 6$ to 8).

p38 and Smad signaling, altogether supporting a program of increased protein synthesis and muscle growth.

Compensatory increases in S6K and FoxO signaling in Nur77-deficient muscle. Having demonstrated that Nur77 overexpression increased Akt/S6K and FoxO3a activity, we proceeded to test if these signaling pathways are downregulated in Nur77-null mice. Akt phosphorylation was unaffected in global Nur77-null muscle (Fig. 8). Contrary to our expectations, however, we observed increased phosphorylation of mTOR (Ser2448), P70S6K (Thr389), and S6 (Ser235). Similar increases in P70S6K and S6 phosphorylation were observed in mDKO mice (Fig. 9A and B). In addition, p-FoxO1 increased and p-FoxO3A tended to increase in muscle lysates from global Nur77-null mice (Fig. 8). The phosphorylation states of p38 and p42/p44 MAPKs were unchanged (data not shown). We observed no difference in p-Smad2/3 (as a percentage of total Smad2/3). However, there was an increase in p-Smad2 when the amount was normalized to the P84 loading control, likely as a result of a trend toward increased total Smad2. With the exception of a trend toward increased p-Smad2 signaling, the remainder of the biochemical changes seen in the Nur77-null mice is predicted to increase muscle growth. In the context of

reduced muscle mass of global Nur77$^{-/-}$ and mDKO mice, however, we reasoned that these signaling changes represent adaptive responses to the developmental loss of IGF1 and consequent muscle hypotrophy. To address this possibility, we compared S6K signaling between 3-week- and 3-month-old mNur77$^{-/-}$ mice. At 3 weeks of age, mNur77$^{-/-}$ mice exhibited reduced body mass and muscle mass (Fig. 9C to G) but no change in the level of S6 phosphorylation, likely due to the high endogenous IGF1 level normally found in young animals (Fig. 9H to I). By 3 months of age, however, there was a robust upregulation of S6 phosphorylation (Fig. 9J to K), consistent with compensatory feedback from other mitogenic pathways, presumably in an effort to promote protein synthesis and muscle growth.

DISCUSSION

In this study, we performed differential expression analysis to identify novel transcriptional programs regulated by Nur77 in skeletal muscle. Using this unbiased approach, we identified changes in genes involved in muscle development and growth, implicating Nur77 as a regulator of muscle mass. Using both gain- and loss-of-function mouse models, we demonstrated that Nur77
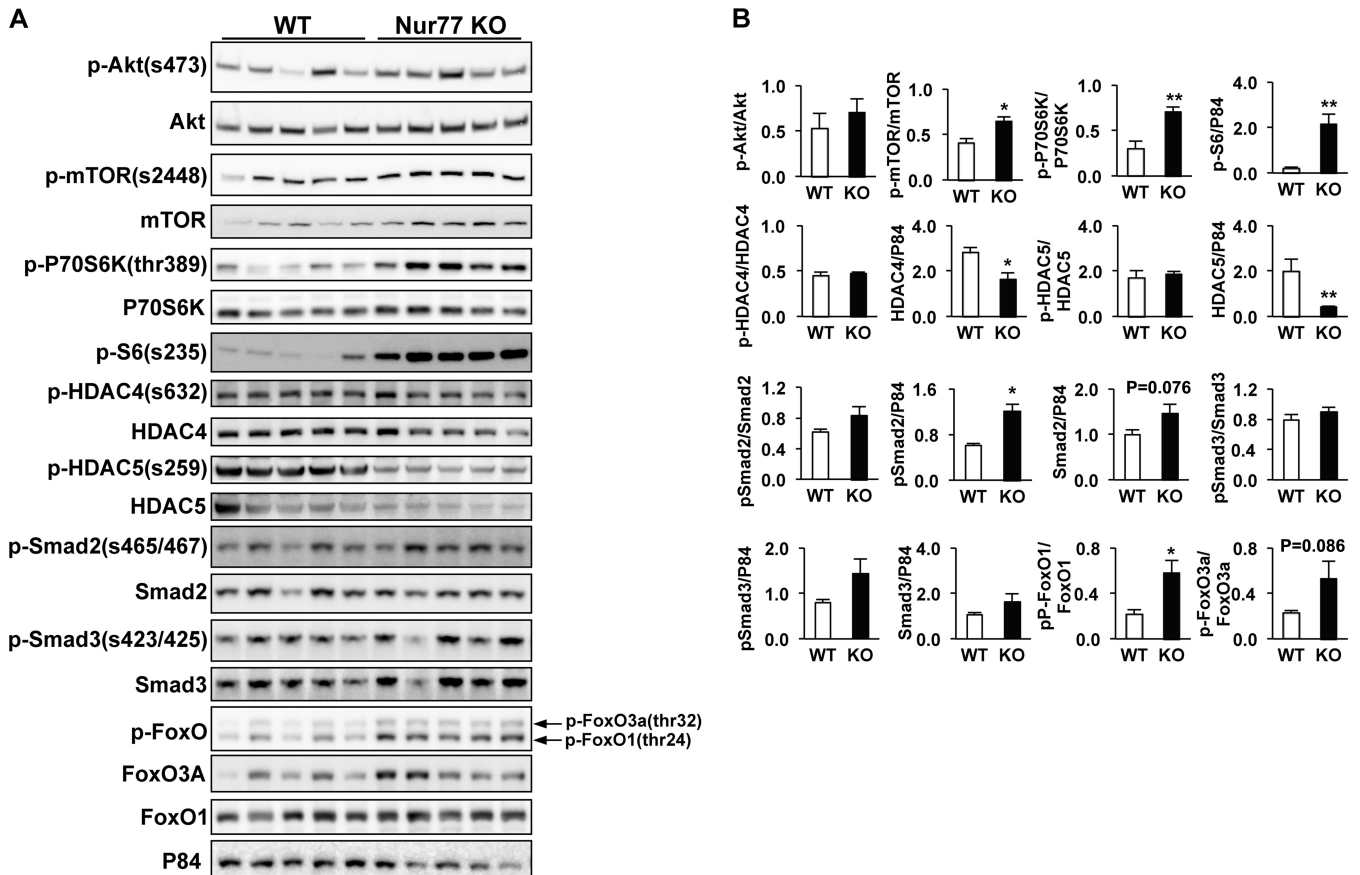
FIG 8 Nur77 deficiency increased Smad2 activity and led to compensatory upregulation of mTOR-S6K and FoxO1 signaling. (A) Immunoblot analysis of total lysates prepared from white quadriceps muscle of male 4-month-old global Nur77 knockout (KO) mice. (B) Densitometry quantification of the results from panel A. *, $P < 0.05$; **, $P < 0.01$ ($n = 6$ to 8).

modulates muscle fiber size by upregulating the expression of IGF1 while simultaneously downregulating the expression of growth-limiting genes such as those for myostatin, Trim63 (MuRF1), and Fbxo32 (MAFbx). In the MCK-Nur77 transgenic mouse, Nur77 upregulation of IGF1 led to changes in Akt-S6K, p38, and p42 MAPK signaling supportive of muscle growth (Fig. 10). Likely as a result of increased Akt activity, transgenic muscle lysates also exhibited increased p-FoxO3A, effectively sequestering FoxO3A in the cytoplasm and reducing its transcriptional activity on targets such as Trim63 and Fbxo32. Concurrently, Nur77-mediated downregulation of myostatin attenuated Smad2/3 signaling, limiting its inhibitory input to Akt. In the Nur77-deficient mice, our findings support a model in which a developmental deficit in IGF1 level contributed to a decrease in muscle mass and fiber size, with an adaptive increase in Akt-S6K and FoxO signaling. Our hypothesis that IGF1 is a downstream mediator of Nur77 is further supported by our findings that manipulating IGF1 level is sufficient to attenuate Nur77's effect on myotube size *in vitro*. Finally, despite prior observations that Nur77 and NOR1 can have redundant activities in certain contexts (18, 53), we find that Nur77, not NOR1, is the dominant NR4A receptor that controls muscle mass.

In the muscle-specific Nur77-overexpressing mice, we observed a pronounced suppression of genes classically induced in muscle atrophy, including those for myostatin, Fbxo32, and

Trim63. In addition, the expression of several other genes more recently implicated in the pathogenesis of muscle atrophy, those for Tnfrsf12a (also known as the TWEAK receptor) and another F-box protein, Fbxo40, was similarly reduced in Nur77 transgenic muscle (Fig. 4) (38, 41, 54). These results suggest that one mechanism by which Nur77 supports myofiber growth is by global suppression of transcriptional programs that favor muscle breakdown. At least in the case of Trim 63 and Fbxo32, this effect appears to be mediated indirectly through IGF1/Akt-mediated inactivation of FoxO3A. The downregulation of Fbxo32 may also result from reduced p38 signaling, which has been shown to drive Fbxo32 expression in cardiac myofibers (45). It is currently unknown whether the expression of TWEAK receptor and Fbxo40 is also regulated by FoxO. Moreover, the mechanism by which Nur77 downregulates myostatin expression remains unclear.

In skeletal muscle, HDAC4 and HDAC5 are well-characterized repressors of MEF2 transcriptional activities. Phosphorylation of these class IIa HDACs by kinases (including CaMK and protein kinase D) promotes nuclear efflux, which relieves their repressive effect on MEF2 target genes to promote myogenesis and muscle hypertrophy (50, 51, 55, 56). That we observed increased "active" HDAC4, in the form of increased total HDAC4 and decreased p-HDAC4, in the MCK-Nur77 transgenic mouse is thus unanticipated. In addition to CaMKII-driven nuclear export, however,
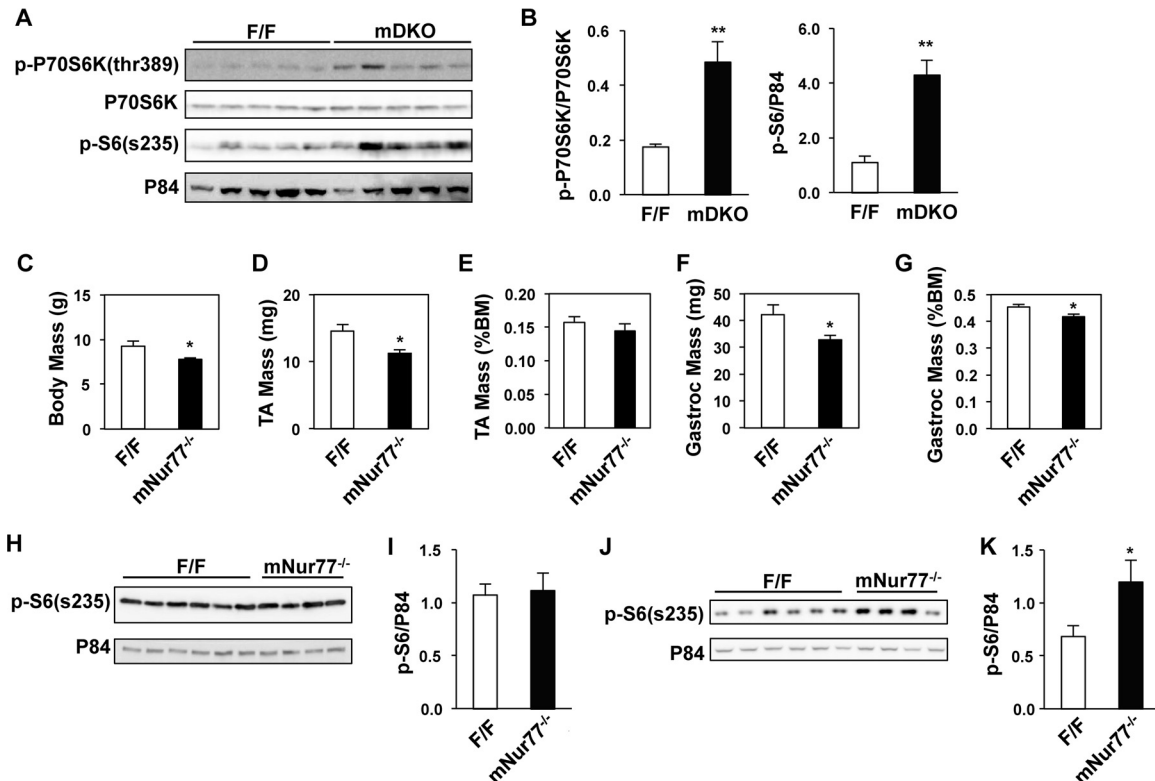
FIG 9 Nur77-deficiency does not induce S6K signaling in young mice. (A and B) Immunoblot and densitometry quantification of S6K signaling in control (flox/flox [F/F]) and muscle-specific Nur77$^{-/-}$/NOR1$^{-/-}$ compound mutant (mDKO) white gastrocnemius muscle lysate. Seven 3-month-old male mice were used. (C to G) Body mass and tibialis anterior (TA) and gastrocnemius (gastroc) mass of 3-week-old female control (F/F) and muscle-specific Nur77-deficient (mNur77$^{-/-}$) mice. (H to K) Immunoblot analysis of S6 phosphorylation from 3-week-old (H and I) and 3-month-old (J and K) flox/flox and mNur77$^{-/-}$ quadricep muscle lysate. For panels H and I $n = 4$ to 6; for panels J and K, $n = 7$. *, $P < 0.05$; **, $P < 0.01$.
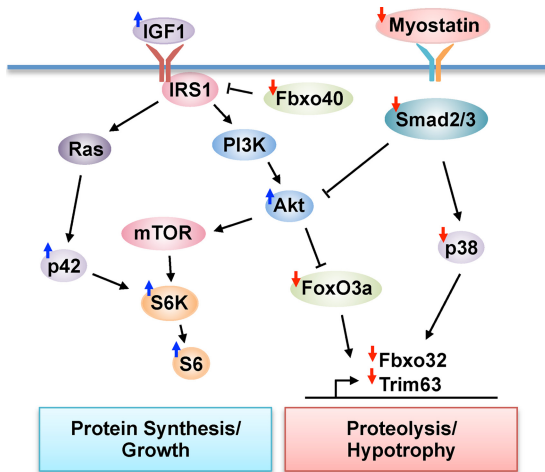

FIG 10 Model for Nur77 regulation of muscle growth. Proteins/genes up-regulated by Nur77 are marked with blue arrows, whereas those downregulated are marked with red arrows. We propose that Nur77's dominant effect on muscle growth is mediated by its effect through IGF1 and myostatin. IGF1 activation increases phosphatidylinositol 3-kinase (PI3K)/Akt signaling and enhances S6K activity to augment protein translation. S6K also receives positive input from p42 MAPK, another downstream effector of IGF1 signaling. Activated Akt also inhibits FoxO3a activity, diminishing its transcriptional activation of atrogenes encoding Fbxo32 and Trim63. Nur77-mediated downregulation of myostatin attenuates Smad2/3 signaling, limiting Smad2/3's inhibition of Akt. Reduced Smad2/3 activity also blunts p38 MAPK activity, which has been shown to be a regulator or Fbxo32 expression. Nur77 also downregulates Fbxo40, which is expected to minimize degradation of IRS1 and inhibition of IGF1 signaling.

HDAC4 is subject to additional levels of regulations in different physiological settings. For instance, Backs et al. have shown that protein kinase A (PKA) activation leads to the generation of an active ~28-kDa N terminus HDAC4 product that can repress MEF2 activity in cardiomyocytes (57). Liu and Schneider similarly reported that PKA phosphorylation at Ser265/266 of HDAC4 and Ser280 of HDAC5 favors nuclear retention of HDAC4/5 and antagonizes CaMKII-mediated nuclear efflux of HDAC4/5 in isolated muscle fibers (58). Collectively, these findings support a model in which HDAC4 integrates physiologic signaling downstream of CaMKII and PKA (57, 58). In this scheme, acute β-adrenergic stimulation (such as in activation of the sympathetic nervous system) would stimulate PKA-mediated HDAC4 retention to redirect energy from myogenesis toward meeting the energetic demand of the actively contracting muscle. Under conditions of sustained stress (such as in physical exercise), adenylyl cyclase activity is uncoupled from the β-adrenergic receptor, leading to diminished cAMP and PKA inactivation (57). In turn, CaMKII activity increases to phosphorylate and inactivate HDAC4, promoting MEF2 activity and muscle hypertrophy. We previously proposed Nur77 as a mediator of the fight-or-flight response based on its rapid transcriptional response to β-adrenergic stimulation and the metabolic program it controls (18). In this context, it is reasonable to consider the increased abundance of active HDAC4 [decreased p-HDAC4 (Ser632)] in the MCK-Nur77 transgenic mouse as a response to PKA activation although the

mechanism by which Nur77 alters HDAC abundance remains to be explored.

Our finding that Nur77 deficiency results in loss of muscle mass in mice as young as 3 weeks of age strongly suggests that Nur77 is an important regulator of muscle development. Several lines of evidence that support Nur77 as a modulator of muscle development. First, Nur77 gene expression is robustly induced during myoblast differentiation in both C2C12 myoblasts and primary murine myoblasts ([59]; our unpublished results). In addition, Nur77 not only regulates the expression of IGF1 but also modulates the transcriptional programming of multiple developmental genes, including those for the fetal growth factor IGF2, and Myh8 (perinatal myosin heavy chain), Myh3 (embryonic myosin heavy chain), and Myl4 (embryonic and atrial myosin light chain) in the MCK-Nur77 transgenic mouse model. Future studies will need to address the importance of Nur77 in postnatal muscle growth. As much of the transcriptional program that occurs during developmental myogenesis is recapitulated in adult muscle regeneration ([60]), our findings raise the question of whether Nur77 also plays a role in modulating muscle regeneration in response to injury. And, if so, does this change stem from its role in satellite cells (muscle progenitor cells) or in differentiating myoblasts? As a requisite of muscle differentiation is cell cycle exit, future studies would also need to examine Nur77's control of cellular proliferation and cyclin-dependent kinase activities. This would be of particular relevance, given our previous work implicating Nur77 in the regulation of cell cycle in adipocytes and beta cells ([61], [62]). In addition, we will need to evaluate the function of Nur77 in the maintenance of adult muscle mass. The generation of inducible Nur77 mouse models will be needed to address this question.

Our *in vivo* and *in vitro* data demonstrating a clear association between Nur77 expression and myofiber size, in the context of transcriptional and biochemical changes supporting protein synthesis and muscle hypertrophy, establish Nur77 as a novel determinant of muscle growth. It remains unclear, however, why Nur77 overexpression does not increase actual muscle mass. We speculate that the most plausible explanation is an adaptive reduction in total myofiber count. Although we were unable to detect differences in fiber number in the Nur77 transgenic EDL, we cannot exclude the possibility of decreased fiber count in other muscles. Due to the nonlongitudinal alignment of most other muscles, accurate determination of total fiber number is technically challenging. Our findings here also imply, however, there may be physiological responses that prevent muscle overgrowth in response to Nur77 overexpression. For instance, the increased abundance of total HDAC4 and reduction in HDAC4 phosphorylation may represent such an attempt to counteract the trophic effects of Nur77.

In summary, our past work and the results presented here lead us to advance the notion that muscle Nur77 expression exerts differential effects according to developmental stages. The MCK-Nur77 transgenic mouse has provided us glimpses into the transcriptional and biochemical programs Nur77 may regulate during developmental myogenesis. We propose that Nur77 complements other muscle regulatory factors in determining muscle mass during developmental myogenesis. Congenital deletion of Nur77 triggers adaptive activation of signaling pathways involved in muscle hypertrophy to compensate for muscle hypotrophy. In adulthood, Nur77 mediates the metabolic response downstream of β-adrenergic stimulation in driving muscle glycolysis and glucose utilization ([18]). It remains to be determined whether Nur77 plays a role in controlling muscle mass during adulthood in the setting of regeneration and exercise-induced muscle hypertrophy. Finally, Nur77's dual role in regulating metabolism and muscle mass raises intriguing questions regarding the interdependence of these two processes. Based on studies examining the impact of nutrition on muscle stem cell function ([63], [64]), we posit that Nur77 coordinates the cross talk between myogenesis and metabolism. Future studies examining the interplay between Nur77, glycolysis, and myogenesis will provide valuable insights into the relationship between metabolism and function, with important implications for conditions such as diabetes and muscle wasting.

ACKNOWLEDGMENTS

REFERENCES

1. **von Haehling S, Anker SD.** 2012. Cachexia as major underestimated unmet medical need: facts and numbers. Int J Cardiol **161**:121–123. http://dx.doi.org/10.1016/j.ijcard.2012.09.213.
2. **Srikanthan P, Hevener AL, Karlamangla AS.** 2010. Sarcopenia exacerbates obesity-associated insulin resistance and dysglycemia: findings from the National Health and Nutrition Examination Survey III. PLoS One **5**:e10805. http://dx.doi.org/10.1371/journal.pone.0010805.
3. **Srikanthan P, Karlamangla AS.** 2011. Relative muscle mass is inversely associated with insulin resistance and prediabetes. Findings from the third National Health and Nutrition Examination Survey. J Clin Endocrinol Metab **96**:2898–2903. http://dx.doi.org/10.1210/jc.2011-0435.
4. **Bauman WA, Spungen AM.** 1994. Disorders of carbohydrate and lipid metabolism in veterans with paraplegia or quadriplegia: a model of premature aging. Metabolism **43**:749–756. http://dx.doi.org/10.1016/0026-0495(94)90126-0.
5. **Ryall JG, Church JE, Lynch GS.** 2010. Novel role for ss-adrenergic signalling in skeletal muscle growth, development and regeneration. Clin Exp Pharmacol Physiol **37**:397–401. http://dx.doi.org/10.1111/j.1440-1681.2009.05312.x.
6. **Egerman MA, Glass DJ.** 2014. Signaling pathways controlling skeletal muscle mass. Crit Rev Biochem Mol Biol **49**:59–68. http://dx.doi.org/10.3109/10409238.2013.857291.
7. **Gundersen K.** 2011. Excitation-transcription coupling in skeletal muscle: the molecular pathways of exercise. Biol Rev Camb Philos Soc **86**:564–600. http://dx.doi.org/10.1111/j.1469-185X.2010.00161.x.
8. **Duchene S, Audouin E, Crochet S, Duclos MJ, Dupont J, Tesseraud S.** 2008. Involvement of the ERK1/2 MAPK pathway in insulin-induced S6K1 activation in avian cells. Domest Anim Endocrinol **34**:63–73. http://dx.doi.org/10.1016/j.domaniend.2006.11.001.
9. **Haddad F, Adams GR.** 2004. Inhibition of MAP/ERK kinase prevents IGF-I-induced hypertrophy in rat muscles. J Appl Physiol **96**:203–210. http://dx.doi.org/10.1152/japplphysiol.00856.2003.
10. **Ryder JW, Fahlman R, Wallberg-Henriksson H, Alessi DR, Krook A, Zierath JR.** 2000. Effect of contraction on mitogen-activated protein kinase signal transduction in skeletal muscle. Involvement off the mitogen- and stress-activated protein kinase 1. J Biol Chem **275**:1457–1462. http://dx.doi.org/10.1074/jbc.275.2.1457.
11. **Egan B, Carson BP, Garcia-Roves PM, Chibalin AV, Sarsfield FM, Barron N, McCaffrey N, Moyna NM, Zierath JR, O'Gorman DJ.** 2010. Exercise intensity-dependent regulation of peroxisome proliferator-activated receptor γ coactivator-1α mRNA abundance is associated with differential activation of upstream signalling kinases in human skeletal muscle. J Physiol **588**:1779–1790. http://dx.doi.org/10.1113/jphysiol.2010.188011.
12. **Ruas JL, White JP, Rao RR, Kleiner S, Brannan KT, Harrison BC, Greene NP, Wu J, Estall JL, Irving BA, Lanza IR, Rasbach KA, Okutsu M, Nair KS, Yan Z, Leinwand LA, Spiegelman BM.** 2012. A PGC-1α

isoform induced by resistance training regulates skeletal muscle hypertrophy. Cell 151:1319–1331. http://dx.doi.org/10.1016/j.cell.2012.10.050.

13. Ruegg MA, Glass DJ. 2011. Molecular mechanisms and treatment options for muscle wasting diseases. Annu Rev Pharmacol Toxicol 51:373–395. http://dx.doi.org/10.1146/annurev-pharmtox-010510-100537.

14. McFarlane C, Plummer E, Thomas M, Hennebry A, Ashby M, Ashby M, Ling N, Smith H, Sharma M, Kambadur R. 2006. Myostatin induces cachexia by activating the ubiquitin proteolytic system through an NF-κB-independent, FoxO1-dependent mechanism. J Cell Physiol 209:501–514. http://dx.doi.org/10.1002/jcp.20757.

15. Stitt TN, Drujan D, Clarke BA, Panaro F, Timofeyva Y, Kline WO, Gonzalez M, Yancopoulos GD, Glass DJ. 2004. The IGF-1/PI3K/Akt pathway prevents expression of muscle atrophy-induced ubiquitin ligases by inhibiting FOXO transcription factors. Mol Cell 14:395–403. http://dx.doi.org/10.1016/S1097-2765(04)00211-4.

16. Helbling JC, Minni AM, Pallet V, Moisan MP. 2014. Stress and glucocorticoid regulation of NR4A genes in mice. J Neurosci Res 92:825–834. http://dx.doi.org/10.1002/jnr.23366.

17. Maxwell MA, Muscat GE. 2006. The NR4A subgroup: immediate early response genes with pleiotropic physiological roles. Nucl Recept Signal 4:e002. http://dx.doi.org/10.1621/nrs.04002.

18. Chao LC, Zhang Z, Pei L, Saito T, Tontonoz P, Pilch PF. 2007. Nur77 coordinately regulates expression of genes linked to glucose metabolism in skeletal muscle. Mol Endocrinol 21:2152–2163. http://dx.doi.org/10.1210/me.2007-0169.

19. Mahoney DJ, Parise G, Melov S, Safdar A, Tarnopolsky MA. 2005. Analysis of global mRNA expression in human skeletal muscle during recovery from endurance exercise. FASEB J 19:1498–1500. http://dx.doi.org/10.1096/fj.04-3149fje.

20. Chao LC, Wroblewski K, Zhang Z, Pei L, Vergnes L, Ilkayeva OR, Ding SY, Reue K, Watt MJ, Newgard CB, Pilch PF, Hevener AL, Tontonoz P. 2009. Insulin resistance and altered systemic glucose metabolism in mice lacking Nur77. Diabetes 58:2788–2796. http://dx.doi.org/10.2337/db09-0763.

21. Chao LC, Wroblewski K, Ilkayeva OR, Stevens RD, Bain J, Meyer GA, Schenk S, Martinez L, Vergnes L, Narkar VA, Drew BG, Hong C, Boyadjian R, Hevener AL, Evans RM, Reue K, Spencer MJ, Newgard CB, Tontonoz P. 2012. Skeletal muscle Nur77 expression enhances oxidative metabolism and substrate utilization. J Lipid Res 53:2610–2619. http://dx.doi.org/10.1194/jlr.M029355.

22. Pearen MA, Eriksson NA, Fitzsimmons RL, Goode JM, Martel N, Andrikopoulos S, Muscat GE. 2012. The nuclear receptor, Nor-1, markedly increases type II oxidative muscle fibers and resistance to fatigue. Mol Endocrinol 26:372–384. http://dx.doi.org/10.1210/me.2011-1274.

23. Sekiya T, Kashiwagi I, Yoshida R, Fukaya T, Morita R, Kimura A, Ichinose H, Metzger D, Chambon P, Yoshimura A. 2013. Nr4a receptors are essential for thymic regulatory T cell development and immune homeostasis. Nat Immunol 14:230–237. http://dx.doi.org/10.1038/ni.2520.

24. Ponnio T, Burton Q, Pereira FA, Wu DK, Conneely OM. 2002. The nuclear receptor Nor-1 is essential for proliferation of the semicircular canals of the mouse inner ear. Mol Cell Biol 22:935–945. http://dx.doi.org/10.1128/MCB.22.3.935-945.2002.

25. Chao LC, Soto E, Hong C, Ito A, Pei L, Chawla A, Conneely OM, Tangirala RK, Evans RM, Tontonoz P. 2013. Bone marrow NR4A expression is not a dominant factor in the development of atherosclerosis or macrophage polarization in mice. J Lipid Res 54:806–815. http://dx.doi.org/10.1194/jlr.M034157.

26. Rando TA, Blau HM. 1994. Primary mouse myoblast purification, characterization, and transplantation for cell-mediated gene therapy. J Cell Biol 125:1275–1287. http://dx.doi.org/10.1083/jcb.125.6.1275.

27. Frey N, Frank D, Lippl S, Kuhn C, Kogler H, Barrientos T, Rohr C, Will R, Muller OJ, Weiler H, Bassel-Duby R, Katus HA, Olson EN. 2008. Calsarcin-2 deficiency increases exercise capacity in mice through calcineurin/NFAT activation. J Clin Invest 118:3598–3608. http://dx.doi.org/10.1172/JCI36277.

28. Lach-Trifilieff E, Minetti GC, Sheppard K, Ibebunjo C, Feige JN, Hartmann S, Brachat S, Rivet H, Koelbing C, Morvan F, Hatakeyama S, Glass DJ. 2014. An antibody blocking activin type II receptors induces strong skeletal muscle hypertrophy and protects from atrophy. Mol Cell Biol 34:606–618. http://dx.doi.org/10.1128/MCB.01307-13.

29. Pearen MA, Goode JM, Fitzsimmons RL, Eriksson NA, Thomas GP, Cowin GJ, Wang SC, Tuong ZK, Muscat GE. 2013. Transgenic muscle-specific Nor-1 expression regulates multiple pathways that effect adipos-

ity, metabolism, and endurance. Mol Endocrinol 27:1897–1917. http://dx.doi.org/10.1210/me.2013-1205.

30. Pei L, Waki H, Vaitheesvaran B, Wilpitz DC, Kurland IJ, Tontonoz P. 2006. NR4A orphan nuclear receptors are transcriptional regulators of hepatic glucose metabolism. Nat Med 12:1048–1055. http://dx.doi.org/10.1038/nm1471.

31. Musaro A, McCullagh K, Paul A, Houghton L, Dobrowolny G, Molinaro M, Barton ER, Sweeney HL, Rosenthal N. 2001. Localized Igf-1 transgene expression sustains hypertrophy and regeneration in senescent skeletal muscle. Nat Genet 27:195–200. http://dx.doi.org/10.1038/84839.

32. Stewart CE, Pell JM. 2010. Point:counterpoint: IGF is/is not the major physiological regulator of muscle mass. Point: IGF is the major physiological regulator of muscle mass. J Appl Physiol 108:1820–1824. http://dx.doi.org/10.1152/japplphysiol.01246.2009.

33. Shavlakadze T, Davies M, White JD, Grounds MD. 2004. Early regeneration of whole skeletal muscle grafts is unaffected by overexpression of IGF-1 in MLC/mIGF-1 transgenic mice. J Histochem Cytochem 52:873–883. http://dx.doi.org/10.1369/jhc.3A6177.2004.

34. Kardon G, Heanue TA, Tabin CJ. 2002. Pax3 and Dach2 positive regulation in the developing somite. Dev Dyn 224:350–355. http://dx.doi.org/10.1002/dvdy.10107.

35. Baehr LM, Furlow JD, Bodine SC. 2011. Muscle sparing in muscle RING finger 1 null mice: response to synthetic glucocorticoids. J Physiol 589:4759–4776. http://dx.doi.org/10.1113/jphysiol.2011.212845.

36. Bodine SC, Latres E, Baumhueter S, Lai VK, Nunez L, Clarke BA, Poueymirou WT, Panaro FJ, Na E, Dharmarajan K, Pan ZQ, Valenzuela DM, DeChiara TM, Stitt TN, Yancopoulos GD, Glass DJ. 2001. Identification of ubiquitin ligases required for skeletal muscle atrophy. Science 294:1704–1708. http://dx.doi.org/10.1126/science.1065874.

37. Labeit S, Kohl CH, Witt CC, Labeit D, Jung J, Granzier H. 2010. Modulation of muscle atrophy, fatigue and MLC phosphorylation by MuRF1 as indicated by hindlimb suspension studies on MuRF1-KO mice. J Biomed Biotechnol 2010:693741. http://dx.doi.org/10.1155/2010/693741.

38. Bhatnagar S, Mittal A, Gupta SK, Kumar A. 2012. TWEAK causes myotube atrophy through coordinated activation of ubiquitin-proteasome system, autophagy, and caspases. J Cell Physiol 227:1042–1051. http://dx.doi.org/10.1002/jcp.22821.

39. McPherron AC, Lawler AM, Lee SJ. 1997. Regulation of skeletal muscle mass in mice by a new TGF-beta superfamily member. Nature 387:83–90. http://dx.doi.org/10.1038/387083a0.

40. Shi J, Luo L, Eash J, Ibebunjo C, Glass DJ. 2011. The SCF-Fbxo40 complex induces IRS1 ubiquitination in skeletal muscle, limiting IGF1 signaling. Dev Cell 21:835–847. http://dx.doi.org/10.1016/j.devcel.2011.09.011.

41. Ye J, Zhang Y, Xu J, Zhang Q, Zhu D. 2007. FBXO40, a gene encoding a novel muscle-specific F-box protein, is upregulated in denervation-related muscle atrophy. Gene 404:53–60. http://dx.doi.org/10.1016/j.gene.2007.08.020.

42. Gomes AV, Waddell DS, Siu R, Stein M, Dewey S, Furlow JD, Bodine SC. 2012. Upregulation of proteasome activity in muscle RING finger 1-null mice following denervation. FASEB J 26:2986–2999. http://dx.doi.org/10.1096/fj.12-204495.

43. Ovcharenko I, Nobrega MA, Loots GG, Stubbs L. 2004. ECR Browser: a tool for visualizing and accessing data from comparisons of multiple vertebrate genomes. Nucleic Acids Res 32:W280–W286. http://dx.doi.org/10.1093/nar/gkh355.

44. Dinchuk JE, Cao C, Huang F, Reeves KA, Wang J, Myers F, Cantor GH, Zhou X, Attar RM, Gottardis M, Carboni JM. 2010. Insulin receptor (IR) pathway hyperactivity in IGF-IR null cells and suppression of downstream growth signaling using the dual IGF-IR/IR inhibitor, BMS-754807. Endocrinology 151:4123–4132. http://dx.doi.org/10.1210/en.2010-0032.

45. Yamamoto Y, Hoshino Y, Ito T, Nariai T, Mohri T, Obana M, Hayata N, Uozumi Y, Maeda M, Fujio Y, Azuma J. 2008. Atrogin-1 ubiquitin ligase is upregulated by doxorubicin via p38-MAP kinase in cardiac myocytes. Cardiovasc Res 79:89–96. http://dx.doi.org/10.1093/cvr/cvn076.

46. Li J, Johnson SE. 2006. ERK2 is required for efficient terminal differentiation of skeletal myoblasts. Biochem Biophys Res Commun 345:1425–1433. http://dx.doi.org/10.1016/j.bbrc.2006.05.051.

47. Sarbassov DD, Jones LG, Peterson CA. 1997. Extracellular signal-regulated kinase-1 and -2 respond differently to mitogenic and differentiative signaling pathways in myoblasts. Mol Endocrinol 11:2038–2047. http://dx.doi.org/10.1210/mend.11.13.0036.

48. **Plaisance I, Morandi C, Murigande C, Brink M.** 2008. TNF-alpha increases protein content in C2C12 and primary myotubes by enhancing protein translation via the TNF-R1, PI3K, and MEK. Am J Physiol Endocrinol Metab **294:**E241–E250. http://dx.doi.org/10.1152/ajpendo.00129.2007.

49. **Backs J, Song K, Bezprozvannaya S, Chang S, Olson EN.** 2006. CaM kinase II selectively signals to histone deacetylase 4 during cardiomyocyte hypertrophy. J Clin Invest **116:**1853–1864. http://dx.doi.org/10.1172/JCI27438.

50. **McKinsey TA, Zhang CL, Lu J, Olson EN.** 2000. Signal-dependent nuclear export of a histone deacetylase regulates muscle differentiation. Nature **408:**106–111. http://dx.doi.org/10.1038/35040593.

51. **McKinsey TA, Zhang CL, Olson EN.** 2000. Activation of the myocyte enhancer factor-2 transcription factor by calcium/calmodulin-dependent protein kinase-stimulated binding of 14-3-3 to histone deacetylase 5. Proc Natl Acad Sci U S A **97:**14400–14405. http://dx.doi.org/10.1073/pnas.260501497.

52. **Trendelenburg AU, Meyer A, Rohner D, Boyle J, Hatakeyama S, Glass DJ.** 2009. Myostatin reduces Akt/TORC1/p70S6K signaling, inhibiting myoblast differentiation and myotube size. Am J Physiol Cell Physiol **296:**C1258–C1270. http://dx.doi.org/10.1152/ajpcell.00105.2009.

53. **Mullican SE, Zhang S, Konopleva M, Ruvolo V, Andreeff M, Milbrandt J, Conneely OM.** 2007. Abrogation of nuclear receptors Nr4a3 and Nr4a1 leads to development of acute myeloid leukemia. Nat Med **13:**730–735. http://dx.doi.org/10.1038/nm1579.

54. **Wu CL, Kandarian SC, Jackman RW.** 2011. Identification of genes that elicit disuse muscle atrophy via the transcription factors p50 and Bcl-3. PLoS One **6:**e16171. http://dx.doi.org/10.1371/journal.pone.0016171.

55. **Lu J, McKinsey TA, Nicol RL, Olson EN.** 2000. Signal-dependent activation of the MEF2 transcription factor by dissociation from histone deacetylases. Proc Natl Acad Sci U S A **97:**4070–4075. http://dx.doi.org/10.1073/pnas.080064097.

56. **Lu J, McKinsey TA, Zhang CL, Olson EN.** 2000. Regulation of skeletal myogenesis by association of the MEF2 transcription factor with class II histone deacetylases. Mol Cell **6:**233–244. http://dx.doi.org/10.1016/S1097-2765(00)00025-3.

57. **Backs J, Worst BC, Lehmann LH, Patrick DM, Jebessa Z, Kreusser MM, Sun Q, Chen L, Heft C, Katus HA, Olson EN.** 2011. Selective repression of MEF2 activity by PKA-dependent proteolysis of HDAC4. J Cell Biol **195:**403–415. http://dx.doi.org/10.1083/jcb.201105063.

58. **Liu Y, Schneider MF.** 2013. Opposing HDAC4 nuclear fluxes due to phosphorylation by β-adrenergic activated protein kinase A or by activity or Epac activated CaMKII in skeletal muscle fibres. J Physiol **591:**3605–3623. http://dx.doi.org/10.1113/jphysiol.2013.256263.

59. **Maxwell MA, Cleasby ME, Harding A, Stark A, Cooney GJ, Muscat GE.** 2005. Nur77 regulates lipolysis in skeletal muscle cells. Evidence for crosstalk between the beta-adrenergic and an orphan nuclear hormone receptor pathway. J Biol Chem **280:**12573–12584. http://dx.doi.org/10.1074/jbc.M409580200.

60. **Grefte S, Kuijpers-Jagtman AM, Torensma R, Von den Hoff JW.** 2007. Skeletal muscle development and regeneration. Stem Cells Dev **16:**857–868. http://dx.doi.org/10.1089/scd.2007.0058.

61. **Chao LC, Bensinger SJ, Villanueva CJ, Wroblewski K, Tontonoz P.** 2008. Inhibition of adipocyte differentiation by Nur77, Nurr1, and Nor1. Mol Endocrinol **22:**2596–2608. http://dx.doi.org/10.1210/me.2008-0161.

62. **Tessem JS, Moss LG, Chao LC, Arlotto M, Lu D, Jensen MV, Stephens SB, Tontonoz P, Hohmeier HE, Newgard CB.** 2014. Nkx6.1 regulates islet beta-cell proliferation via Nr4a1 and Nr4a3 nuclear receptors. Proc Natl Acad Sci U S A **111:**5242–5247. http://dx.doi.org/10.1073/pnas.1320953111.

63. **D'Souza DM, Al-Sajee D, Hawke TJ.** 2013. Diabetic myopathy: impact of diabetes mellitus on skeletal muscle progenitor cells. Front Physiol **4:**379. http://dx.doi.org/10.3389/fphys.2013.00379.

64. **Woo M, Isganaitis E, Cerletti M, Fitzpatrick C, Wagers AJ, Jimenez-Chillaron J, Patti ME.** 2011. Early life nutrition modulates muscle stem cell number: implications for muscle mass and repair. Stem Cells Dev **20:**1763–1769. http://dx.doi.org/10.1089/scd.2010.0349.